

A Study on Pore Size Distribution of Modified Ultrathin Membranes

HARUHIKO OHYA, YUTAKA IMURA,* TOHRU MORIYAMA,†
and MASAO KITAOKA, *Department of Chemical Engineering,*
Yokohama National University, Yokohama, Japan

Synopsis

An equation to estimate the thickness of ultrathin membranes obtained by Levich, assuming constant physical properties, was compared with the measured thickness in the range of 0.3–40 μ . The proportionality constant was found to be 0.4, and the equation is expressed as follows:

$$\bar{\delta}_s = 0.4 \left(\frac{\rho_L}{\rho_s} \right) w_s \sqrt{\frac{\mu u_0}{\rho_L g}}$$

The nitrogen gas adsorption isotherms at -195°C on the modified ultrathin membranes were measured and the surface area of the pores was determined by the B.E.T. equation. Distribution of pore volume was calculated by the method of Cranston and Inkley. On the assumption of straight cylindrical pores in the membrane, the cross-sectional area of pores and the mean pore radius were calculated. Symmetric structure of the modified ultrathin membranes was confirmed by reverse osmosis tests with both the air and glass sides of the membrane facing the pressure solution.

INTRODUCTION

The porous structure of modified cellulose acetate membranes was examined under the electron microscope by Riley et al.^{1,2} They confirmed that the membrane consists of a dense, thin surface layer on the side of the film exposed to air during casting, with a highly porous substructure underneath the surface layer. They reported that the dense surface layer was devoid of structural characteristics and showed no evidence of pores greater than about 100 \AA (20 \AA^3), and has a thickness of about 0.25 μ compared to the total membrane thickness of 100 μ . The thickness of the dense surface layer was also reported to be 0.25 μ by Michaels et al.,⁴ a few microns by Kesting et al.,⁵ and 0.7–0.8 μ by Suzuki et al.⁶

There have been several approaches on the mechanism of reverse osmotic flow of water through the membrane in connection with its structure. Some of these have been discussed extensively by Merten.⁷ Alignment diffusion mechanism is favored by Raid and Breton.^{8,9,10} According to

* Present address: Japan Synthetic Rubber Co., Ltd., Yokkaichi, Mie-ken, Japan.

† Present address: Fuji Kasui Engineering Co. Ltd., Shinagawa, Tokyo, Japan.

this mechanism, the existence of pores in the membrane must be avoided for practical desalination application of reverse osmosis. A solution-diffusion mechanism is favored by Lonsdale et al.,¹¹⁻¹⁵ where transport equations are apparently limited to their concept of perfect membranes, which are presumably those which have a complete nonporous surface structure.¹⁵ Banks and Sharples^{16,17,18} also considered that the mechanism of reverse osmosis is one of diffusion flow through the pore-free layer on the membrane surface.

According to Michaels et al.,¹⁵ water transport in reverse osmosis is by molecular diffusion through the polymer matrix, and solute transport is by parallel mechanism involving sorption, activated diffusion, and hydrodynamic flow. According to Sherwood et al.,²⁰ water and solute cross the membrane by parallel processes of diffusion and pore flow. According to the preferential sorption-capillary flow mechanism by Sourirajan,²¹⁻²⁴ separation by reverse osmosis is the combined result of an interfacial phenomenon and fluid transport under pressure through capillary pores, and the appropriate membrane is a porous medium at all levels of solute separation. Glueckauf²⁵ has put forward recently the most satisfactory explanation of ionic repulsion in membrane pores.

Mears²⁶ estimated the average pore radius as $\sim 9 \text{ \AA}$, and the fraction of the total volume occupied by the pores as 0.04. Agrawal and Sourirajan²⁷ estimated it as $\sim 20 \text{ \AA}$.

Taking these discussions into consideration, it seems inevitably important for the further development of reverse osmosis to decide whether pores exist or not in the dense layer of the membrane by a suitable independent method other than reverse osmosis.

ULTRATHIN MEMBRANES

The ultrathin membrane was considered to consist of only a dense, thin cellulose acetate membrane devoid of porous structure. Merten et al.¹⁵ prepared ultrathin cellulose acetate membranes by the Carnell-Cassidy technique,^{28,29} which consists essentially of slowly withdrawing a clean glass plate from a dilute solution of a polymer in a suitable solvent.

The problem of estimating the steady-state thickness δ of the liquid film that adheres to a flat plate of infinite width drawn vertically at a constant speed u_0 from a liquid bath has been summarized by Tallmadge and Gulfinger,³⁰ and the thickness δ may be expressed as follows:

$$\delta \sim \sqrt{\frac{\mu u_0}{\rho g}} \quad (1)$$

where μ = viscosity of solution, ρ = density of solution, and g = gravitational constant. The proportionality constant is found to be unity for the pure liquid.³⁵ But in the present case, the increase of surface tension at the plate-bulk solution boundary region due to the increase in polymer concentration as a result of solvent evaporation could cause a reduction in the

thickness of polymer solution on a flat plate, and hence the proportionality constant may be expected to be smaller than unity.

One square centimeter of solution film having an average thickness $\bar{\delta}$ contains the following weight of cellulose acetate: $\bar{\delta}\rho_L w_s$. After the solvent evaporates completely, the average thickness of cellulose acetate film $\bar{\delta}_s$ may be expressed dividing this weight by the density of cellulose acetate film ρ_s :

$$\bar{\delta}_s = \frac{\rho_L}{\rho_s} w_s \bar{\delta} \quad (2)$$

where ρ_L , and ρ_s = density of the solution and cellulose acetate, respectively, w_s = weight fraction of the cellulose acetate in solution, and $\bar{\delta}$ = average thickness of solution.

Experimental Membrane Thickness

Dilute acetone solutions containing 0.03, 0.04, 0.05, 0.06, 0.10, and 0.20 g cellulose acetate (E398-3 supplied by Eastman Chemical Products, Inc.) per 1 cc acetone were prepared by mixing the solutions overnight. Glass plates (150 mm long, 40 mm wide, and 5 mm thick), immersed in solution to 100 mm, were used as the film-forming surfaces. Temperature of the solutions was kept constant at 30°C.

The procedure of casting ultrathin membranes was identical with the method described by Riley et al.¹⁵ The plate withdrawal rate was 0.1 to 0.9 cm/sec. In each case, the evaporation time was 1 min, after which the plate was immersed in ice-cold water. The membrane thickness was determined by weighing the dried membrane, using the membrane surface area, and assuming its density to be 1.3 g/cm³. The results are shown in Table I.

The effect of the acetone evaporation period on the membrane thickness was investigated for a dilute solution of 0.05 g cellulose acetate per 1 cc and a withdrawal rate of 0.224 cm/sec. It was found that the thickness at different periods remained essentially constant, as shown in Figure 1. This means that acetone evaporates within these periods essentially completely, and hence film thickness is independent of evaporation time. The main parameters which affect film thickness are viscosity and density of the solution and withdrawal rate of the plate.

Measured thickness of membranes for five different rates and for six different concentrations was plotted in Figure 2, as a function of $(\rho_L/\rho_s)w_s \sqrt{\mu u_0/\rho_L g}$ following eqs. (1) and (2). The results were found to be in excellent agreement with the expression

$$\bar{\rho}_s = 0.4 \left(\frac{\rho_L}{\rho_s} \right) w_s \sqrt{\frac{\mu u_0}{\rho_L g}} \quad (3)$$

The Modified Ultrathin Membrane

A number of the modified Loeb and Manjikian-type ultrathin membranes were also prepared by almost the same method mentioned above, from

TABLE I
Membrane Thickness and Physical Properties of Casting Solutions at 30°C

Concentration of cellulose acetate in solution, g/l.	w_s	Viscosity, cp	Density, g/cm ³	Withdrawal rate, cm/sec	Membrane thickness, μ	
					Observed	Estimated by eq. (3)
30	0.0367	3.81	0.798	0.20	0.38	0.28
40	0.0485	7.82	0.801	0.20	0.58	0.59
50	0.0599	8.85	0.807	0.20	0.67	0.70
60	0.0709	16.04	0.810	0.20	0.89	1.10
50	0.0599	7.82	0.807	0.90	1.44	1.49
50	0.0599	7.82	0.807	0.45	1.09	1.10
50	0.0599	7.82	0.807	0.225	0.76	0.75
50	0.0599	7.82	0.807	0.112	0.50	0.53
100	0.113	60	0.821	0.90	6.55	7.39
100	0.113	60	0.821	0.45	5.52	5.23
100	0.113	60	0.821	0.225	3.58	3.70
100	0.113	60	0.821	0.112	2.20	2.61
200	0.203	760	0.860	0.90	40.3	48.4
200	0.203	760	0.860	0.45	34.7	34.2
200	0.203	760	0.860	0.225	26.1	24.2
200	0.203	760	0.860	0.112	19.5	17.1

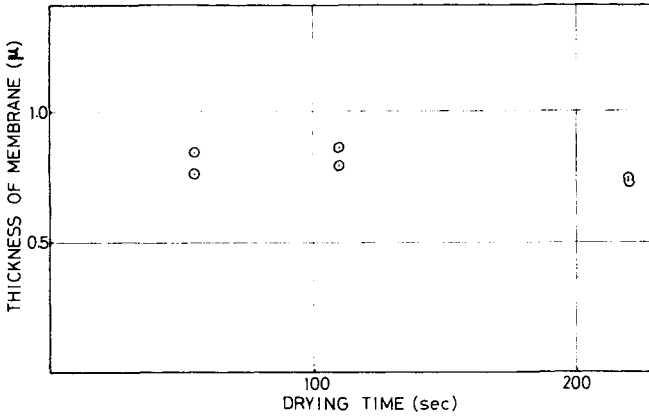


Fig. 1. Measured thickness of ultrathin membranes vs. evaporation time: concentration of cellulose acetate = 0.05 g/cm³ of acetone; withdrawal rate = 0.224 cm/sec.

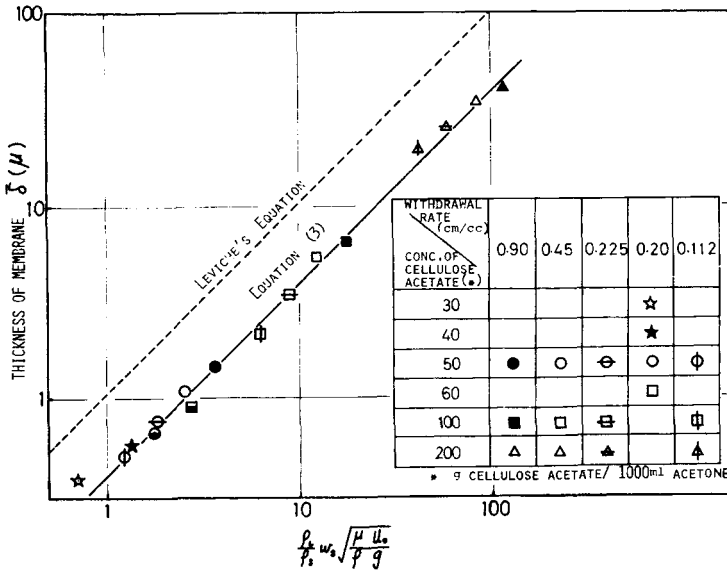


Fig. 2. Measured and predicted thickness of ultrathin membranes.

casting solutions whose compositions are shown in Table II. The evaporation period, however, was 4 min in all cases. Thickness of this modified type may also be expressed by the eq. (3), up to a ratio of 5:10 for cellulose acetate to formamide, using withdrawal rate, physical properties of the solution, and the density of the porous ultrathin membrane $\bar{\rho}_{sm}$, which can be calculated from the B.E.T. plot mentioned later. When the formamide content in the casting solution increases, the thickness of the resulting membrane is lower than that calculated by eq. (3). For example, for the casting solution composition I-7, the actual thickness of the membrane obtained was only 70% of that calculated from eq. (3).

TABLE II
Composition, Physical Properties, Pore Volume, Surface Area, and Reverse Osmotic Characteristics for Each Batch^a

Batch no.	Ratio of cellulose acetate to formamide	Weight fraction of cellulose acetate	Viscosity, cp	Density, g/cm ³	Superficial surface area of membrane, ^b m ² /g	Estimated membrane thickness, μ	Surface area of pores, m ² /g	Flux, g/cm ² ·hr			
								Air side in contact with salt solution	Glass side in contact with salt solution	Air side in contact with salt solution	Glass side in contact with salt solution
I-1	5:0.0	0.04843	4.10	0.8013	0.5958	0.408	0.0	0.067	0.060	95.5	87.5
I-2	5:0.1	0.04839	4.11	0.80223	0.59345	0.4088	8.64	0.109	0.109	89.0	94.5
I-3	5:1	0.04837	4.45	0.80445	0.57141	0.4257	9.88	0.143	—	90.0	—
I-4	5:3	0.04706	31.7	0.80812	0.21954	1.108	13.94	1.10	1.50	47.7	33.4
I-5	5:5	0.04838	4.75	0.81444	0.54953	0.4426	15.81	9.55	9.38	25.5	27.5
I-6	5:10	0.04839	5.42	0.82729	0.51032	0.4767	12.48	*	*	*	*
I-7	5:18	0.04837	6.14	0.84866	0.47361	0.5136	45.3	*	*	*	*

^a The flux and salt rejection data in each case were obtained with different samples of the membrane cast under the same conditions.

^b Assuming $p = 1.3$ g/cm².

^c Indicates that reverse osmotic experiment was not done because membranes were too fragile to be handled.

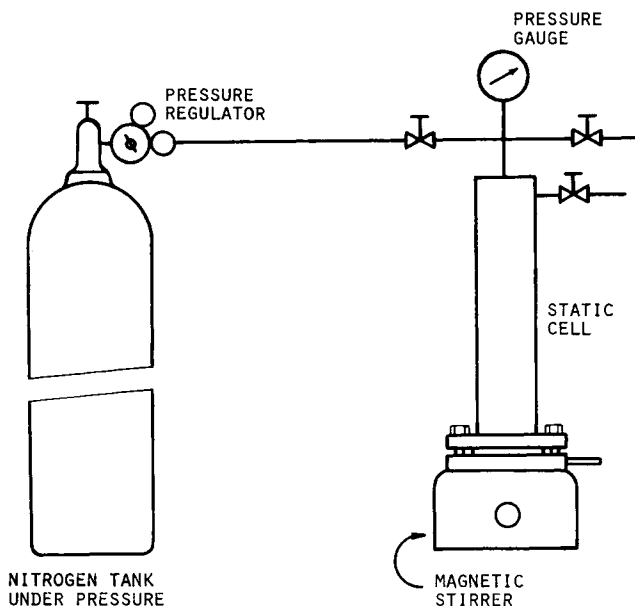


Fig. 3. Reverse osmosis cell assembly.

An acetone evaporation period of 4 min might be enough time to evaporate all acetone in the modified ultrathin membrane, because evaporation of almost all acetone in the ordinary modified membrane (not ultrathin) was already observed during this period.³⁴

The membranes were floated off each surface of the glass plate onto the surface of the water and stored wet. After more than 50 membranes were collected, they were freeze dried as follows. The wet membranes were immersed in a small volume of liquid nitrogen, then frozen and ground to small pieces (5–0.1 mm) to avoid stacking. The freeze-drying process was completed at -5°C over two nights.

The adsorption isotherms of the freeze-dried membrane at -195°C were determined on a standard Emmett and Brunauer apparatus supplied by Shibata Chemical Apparatus Mfg. Co. The gas used was prepurified nitrogen dried through a cold trap cooled to liquid nitrogen temperature.

The reverse osmosis experiment with the modified ultrathin membranes were carried out at laboratory temperature at a pressure of $20\text{ kg/cm}^2\text{G}$, using the reverse osmosis cell shown in Figure 3. The modified ultrathin membranes used were cast on larger glass plates (150 mm long, 70 mm wide, and 5 mm thick) immersed in solution to 70 mm. The cell was a stainless steel pressure chamber consisting of two detachable parts, and the effective membrane area was 9.6 cm^2 . Membrane filters supplied from Toyo Roshi Corp. Ltd. were used as the modified ultrathin membrane support: type TM-5 with mean pore size of $0.1\ \mu$. The modified ultrathin film supported on the membrane filter was mounted on a stainless steel porous plate embedded in the lower part of the cell through which the membrane-permeated liquid was withdrawn at atmospheric pressure. The upper part

TABLE III
Pore size Distributions

Pore size, Å		I-2		I-3		I-4	
Radius range	Average range	Pore volume $\times 10^{-4}$, cm ³ /m ² membrane	Cross-sectional area of pore, cm ² /m ² membrane	Pore volume $\times 10^{-4}$, cm ³ /m ² membrane	Cross-sectional area of pore, cm ² /m ² membrane	Pore volume $\times 10^{-4}$, cm ³ /m ² membrane	Cross-sectional area of pore, cm ² /m ² membrane
35-40	37.5	0.058	1.413	0.152	3.528	0.782	5.430
30-35	32.5	0.150	3.672	0.581	13.651	1.621	11.255
25-30	27.5	0.527	12.877	1.029	24.184	3.272	22.719
22.5-25	23.75	0.901	10.466	1.897	21.172	5.148	16.998
20.0-22.5	21.25	1.906	23.315	3.056	35.899	8.357	17.228
17.5-20	18.75	2.876	35.704	5.902	69.320	11.548	40.083
15-17.5	16.25	3.040	36.991	4.609	55.564	12.958	44.981
12.5-15	13.75	3.008	36.791	2.455	28.840	15.189	56.022
10-12.5	11.25	0.259	3.167			2.769	9.610
Mean pore radius based on							
cross-sectional area		19.753 Å		20.261 Å		19.281 Å	
radius		18.157 Å		19.419 Å		18.401 Å	
Pore size, Å		I-5		I-6		I-7	
Radius range	Average range	Pore volume $\times 10^{-4}$, cm ³ /m ² membrane	Cross-sectional area of pore, cm ² /m ² membrane	Pore volume $\times 10^{-4}$, cm ³ /m ² membrane	Cross-sectional area of pore, cm ² /m ² membrane	Pore volume $\times 10^{-4}$, cm ³ /m ² membrane	Cross-sectional area of pore, cm ² /m ² membrane
35-40	37.5	0.426	9.528	0.505	10.587	0.725	14.118
30-35	32.5	0.643	14.535	1.046	21.945	1.311	25.534
25-30	27.5	1.496	33.803	2.672	56.059	2.144	41.742
22.5-25	23.75	1.921	20.609	6.086	60.648	4.144	38.324
20-22.5	21.25	3.724	42.071	8.471	88.844	7.877	76.606
17.5-20	18.75	5.167	58.366	15.746	165.157	15.248	148.435
15-17.5	16.25	6.591	74.404	10.279	108.815	18.012	175.354
12.5-15	13.75	5.620	63.477	1.011	10.600	12.506	121.694
10-12.5	11.25	0.757	8.549			7.642	74.811
9-10	9.5					6.849	9.891
Mean pore radius based on							
cross-sectional area		19.718 Å		21.038 Å		18.289 Å	
radius		19.003 Å		20.235 Å		16.953 Å	

of the cell contained the feed solution under pressure in contact with the membrane. The two parts of the cell were clamped and sealed tight using rubber O-rings. Compressed nitrogen gas was used to pressurize the system. About 250 cc of the feed sodium chloride solution concentration of which was about 3500 ppm were used each time.

The feed solution was kept well stirred by means of a magnetic stirrer fitted in the cell about 0.5 cm above the membrane surface. The quantity of liquid removed by membrane permeation was small compared to the amount of feed solution in the pressure chamber. The compositions of the feed and the membrane-permeated liquid were computed from the conductivity of these solutions at 25°C as measured by a Radiometer type CDM-3 conductivity meter.

RESULTS AND DISCUSSION

Isotherms of Freeze-Dried Membranes

Figure 4 gives the experimental isotherms of seven kinds of freeze-dried Loeb-Manjikian-type ultrathin membranes at -195°C .

The data of batch I-2 in Figure 4, expressed as B.E.T. plot in Figure 5, yield $2.7 \text{ m}^2/\text{m}^2$ of membrane area for the pore surface area. The latter was estimated from the B.E.T. equation³¹ for the nitrogen isotherm, using 16.2 \AA^2 as the area occupied by each adsorbed nitrogen molecule. Similar calculations were done for batches I-3 to I-7, and the results are shown in Table II.

The ultrathin membrane batch I-1, obtained from the cellulose acetate-acetone solution, was the only one that did not absorb nitrogen at all. This means that the batch I-1-type membrane has no inner surface and that a flat surface does not absorb nitrogen within the pressure range of these experiments.

Pore Size Distributions

The pore size distributions of the freeze-dried membranes were determined by the method of Cranston and Inkley³² using low-temperature adsorption isotherms. The volume of the pores for each pore size range was calculated, and results are shown in Table III.

Assuming that all pores are straight cylindrical, perpendicular to the membrane surface, and that the length of each pore is the same as the thickness of the membrane calculated by eq. (3), the cross-sectional area assigned to pores of each radius was calculated and is shown in Table III.

For batch I-2 (cellulose acetate:formamide = 5:0.1), the total cross-sectional area of pores was 154 cm^2 per m^2 of membrane surface, which corresponds to 1.54% of the membrane surface area. For batch I-3 (cellulose acetate:formamide = 5:1), the total cross-sectional area of pores was 252 cm^2 per m^2 of membrane surface, which corresponds to 2.52% of the membrane surface area. For batch I-1 (cellulose acetate:formamide = 5:0), there was no pore, judging from the isotherm shown in Figure 4.

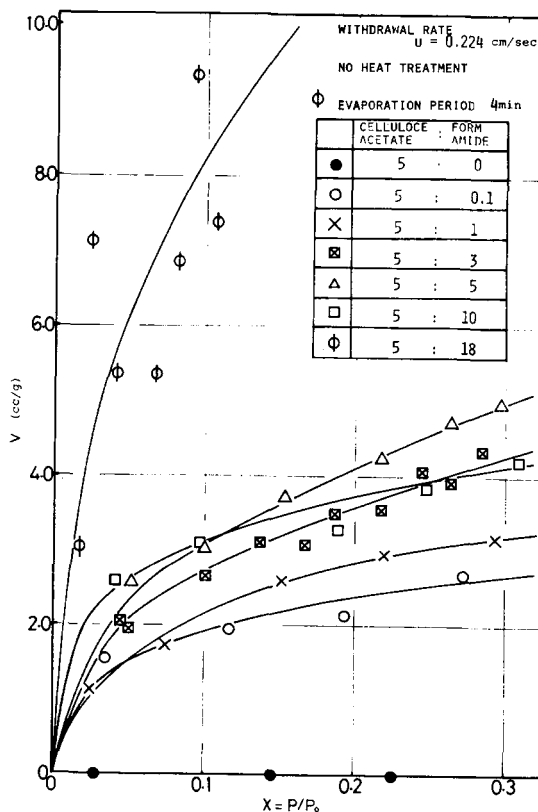


Fig. 4. Nitrogen adsorption isotherms for one ultrathin and five modified ultrathin membranes at -195°C .

The distribution of the cross-sectional area of pores are shown in Figure 6. The mean radii of pores, based on pore cross-sectional area and pore radius, were calculated and are listed in Table III.

The mean radii are similar to that estimated by Agrawal and Sourirajan ($\sim 20 \text{ \AA}$) rather than that by Meares ($\sim 9 \text{ \AA}$). The accuracy of the cross-sectional area of pores depends mostly on the accuracy of the estimation of the membrane thickness and tortuosity. Especially the thickness of the modified ultrathin membrane cast from the solution of 18 parts formamide to 5 parts cellulose acetate was found to be thinner by 70% than estimated by eq. (3). When 10 ml of the solution was mixed well with 1 liter cold water, the dried weight of cellulose acetate collected from the cold water was 0.33 g, compared with 0.41 g estimated from the weight fraction as shown in Table II. The difference might be dissolved into the cold water. This dissolution may be one of the reasons why the thickness of the membrane is thinner than expected.

Reverse Osmosis Separation

Results obtained with batches I-1 to I-5 ultrathin membranes which were used without heat treatment are also presented in Table II. Reverse

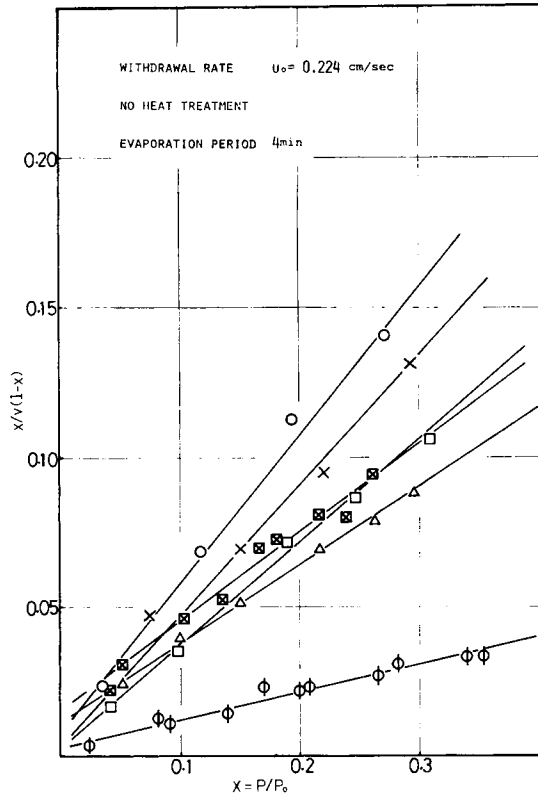


Fig. 5. B.E.T. plots for the adsorption of nitrogen gas on modified ultrathin membranes. Symbols same as shown in Fig. 4.

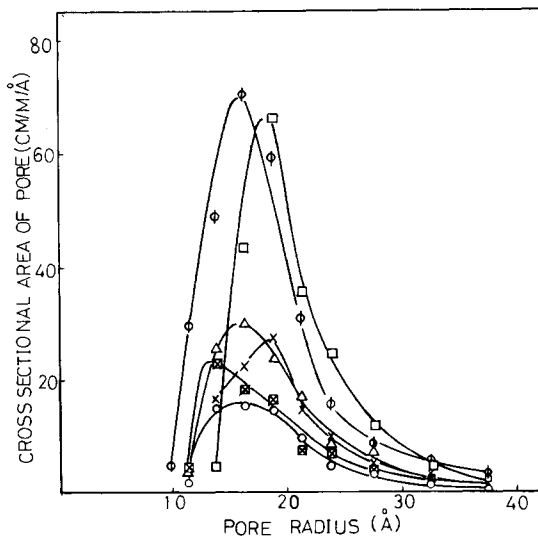


Fig. 6. Distributions of cross-sectional area of pores in ultrathin membranes. Symbols same as shown in Fig. 4.

osmosis tests were done facing both air and glass sides to high-pressure salt solution at 20 kg/cm²G. Compositions I-6 and I-7 yielded membranes which were too fragile to be handled, therefore reverse osmosis experiments were not carried out with these membranes. The reverse osmotic characteristics of the modified ultrathin membranes were found to be almost the same for both sides.

The increase in the amount of formamide in the casting solution corresponds to an exponential increase in water flux through the membrane, as observed by Manjikian,³³ but up to the ratio of cellulose acetate:formamide = 5:1, salt rejection remained constant, and decreased quickly beyond that point.

From the adsorption isotherm shown in Figure 4, there are no pores at all on the ultrathin membrane cast from the solution composed of 40 g cellulose acetate in 1 liter acetone containing no formamide. Its structure is dense and might be assumed to be homogeneous from the same results of the reverse osmosis test for both sides of the membrane. With addition of formamide to the above solution, batches I-2 to I-5 were obtained. The formamide content of the latter solution increased from zero to 5 parts of cellulose acetate. The modified ultrathin membranes cast from the above solutions increased the porous structure of the membranes.

The water flux and salt separation were essentially identical with air side and glass side of the membrane facing the high-pressure solution in all cases. These results show that the porous structure of the membranes used was not asymmetric. Further, it was already shown³⁶ that asymmetry of porous structure would show itself in reverse osmosis experiments at pressure higher than 14 kg/cm². Therefore, it is reasonable to conclude that the porous structure of the membranes used in this work was not asymmetric.

On the basis of the foregoing discussion, the results shown in Table III and Figure 6 indicate that (1) the presence of formamide in the casting solution is responsible for the creation of pores in the resulting membrane, (2) the average size of pores in the membrane is essentially independent of the amount of formamide present in the range of compositions studied in this work, (3) the number of pores in the membrane increases with increase in formamide in the casting solution, and (4) while the assumption of no tortuosity factor overestimates the pore radius, the effect of swelling agent in the casting solution which decreases film thickness underestimates the pore radius as given by the technique described in this paper.

CONCLUSIONS

The results presented in this paper show that the presence of a swelling agent in the casting solution leads to a porous structure in the resulting membranes.

The authors are grateful to Dr. S. Sourirajan for his valuable discussions and H. Konuma and H. Shibuya for their valuable assistance in the progress of these investigations.

References

1. R. L. Riley, J. O. Gardner, and U. Merten, *Science*, **143**, 801 (1964).
2. R. L. Riley, J. O. Gardner, and U. Merten, *Desalination*, **1**, 30 (1966).
3. L. Nakane, S. Suzuki, and S. Ishizaka, 20th Annual Meeting of the Society of Sea Water Science of Japan, Tokyo, 1969.
4. A. S. Micheals, H. J. Bixler, and R. M. Hodges, M.I.T. Dept. of Chem. Eng. Rept. 315-1 DSR 9409, Cambridge, Mass., 1964.
5. R. E. Kesting, M. X. Bursh, and A. L. Vincent, *J. Appl. Polym. Sci.*, **9**, 1873 (1965).
6. T. Kamizawa and S. Isizaka, 19th Annual Meeting of the Society of Sea Water Science of Japan, Tokyo, 1968.
7. U. Merten, in *Desalination by Reverse Osmosis*, U. Merten, Ed., M.I.T. Press, Cambridge, Mass., 1966, Chap. 2.
8. E. J. Breton, Office of Saline Water Research and Development Progress Report No. 16, 1957.
9. E. J. Breton and C. E. Reid, *Chem. Eng. Symp. Ser.*, **24**, 171 (1959).
10. C. E. Reid and E. J. Breton, *J. Appl. Polym. Sci.*, **1**, 133 (1959).
11. H. K. Lonsdale, in *Desalination by Reverse Osmosis*, U. Merten, Ed., M.I.T. Press, Cambridge, Mass., 1966, Chap. 4.
12. H. K. Lonsdale, U. Merten, and R. L. Riley, *J. Appl. Polym. Sci.*, **9**, 1341 (1967).
13. H. K. Lonsdale, U. Merten, R. L. Riley, K. D. Vos, and J. C. Westmoreland, Office of Saline Water Research and Development Progress Report No. 111, 1964.
14. H. K. Lonsdale, U. Merten, and M. Tagami, *J. Appl. Polym. Sci.*, **11**, 1807 (1967).
15. R. L. Riley, H. K. Lonsdale, C. R. Lyons, and U. Merten, *J. Appl. Polym. Sci.*, **11**, 2143 (1967).
16. W. Banks and A. Sharples, *J. Appl. Chem.*, **16**, 28 (1967).
17. W. Banks and A. Sharples, *ibid.*, **16**, 94 (1967).
18. W. Banks and A. Sharples, *ibid.*, **16**, 153 (1967).
19. A. S. Michaels, H. J. Bixler, and R. M. Hodges, *J. Colloid Sci.*, **20**, 1034 (1965).
20. T. K. Sherwood, P. L. T. Brian, and R. E. Fisher, *Ind. Eng. Chem., Fundam.*, **6**, 2 (1967).
21. S. Sourirajan, *Ind. Eng. Chem., Fundam.*, **2**, 51 (1963).
22. S. Sourirajan, in *Water Resources of Canada*, C. E. Dolman, Ed., Univ. of Toronto Press, Toronto, 1967, pp. 154-182.
23. S. Sourirajan, *Can. Sci.*, **1**(3), 22 (1967).
24. S. Sourirajan, *Reverse Osmosis*, Logos Press, London, 1970.
25. E. Glueckauf, *Proc. First International Symposium on Water Desalination, Oct. 3-9, 1965*, Vol. 1, U.S. Dept. of Interior, Office of Saline Water, Washington, D.C., 1967, 143-56.
26. P. Meares, *Eur. Polym. J.*, **2**, 241 (1966).
27. J. P. Agrawal and S. Sourirajan, *J. Appl. Polym. Sci.*, **14**, 1303 (1970).
28. P. H. Carnell and H. G. Cassidy, *J. Polym. Sci.*, **55**, 233 (1961).
29. P. H. Carnell, *Appl. Polym. Sci.*, **9**, 1863 (1965).
30. J. A. Tallmadge and C. Gutfinger, *Ind. Eng. Chem.*, **59**(11), 19, (1967).
31. S. Brunauer, P. H. Emmett, and E. Teller, *J. Amer. Chem. Soc.*, **60**, 309 (1938).
32. R. W. Crauston and F. A. Inkley, *Advan. Catal.*, **9**, 143 (1957).
33. S. Manjikian, *Ind. Eng. Chem., Prod. Res. Develop.*, **6**, 23 (1967).
34. H. Ohya and S. Sourirajan, *J. Appl. Polym. Sci.*, **15**, 705 (1971).
35. V. G. Levich, *Physicochemical Hydrodynamics*, Prentice Hall, New York, 1962, Chap. 12.
36. J. Kopeček and S. Sourirajan, *J. Appl. Polym. Sci.*, **13**, 637 (1969).

Received May 3, 1971

Revised October 12, 1973